Thin-film synthesis of the orthorhombic phase of SnO_2

F. J. Lamelas
Department of Physics, Marquette University, Milwaukee, Wisconsin 53233

S. A. Reid
Department of Chemistry, Marquette University, Milwaukee, Wisconsin 53233

(Received 31 March 1999)

We demonstrate the formation of an SnO_2 thin film in an orthorhombic phase which has previously been found in high-pressure experiments. Our starting point was the pulsed-laser deposition of an amorphous film of SnO on Si [001] substrates. During a series of subsequent heat treatments in air, the film crystallized in a sequence of three phases. First, after heating to 300 °C, the litharge phase of SnO was formed. Next, while heating to 700 °C, the film absorbed oxygen and formed the high-pressure orthorhombic phase of SnO_2. Eventually, after heating to 1150 °C, the film was fully converted to the stable cassiterite phase of SnO_2. The experiments performed to date are not conclusive, but indirect evidence indicates that the litharge structure is important as an intermediary in the formation of the orthorhombic phase, in contrast to the transformation route at high pressure. [S0163-1829(99)10037-7]

I. INTRODUCTION

The most important form of naturally occurring SnO_2 is cassiterite, a phase of SnO_2 with the tetragonal rutile structure.[1] A tetragonal phase of SnO is also stable under ambient conditions, with a structure determined by Moore and Pauling,[2] and refined more recently by Pannetier and Denes[3] and by Izumi.[4] Tetragonal SnO has the same structure as litharge, a mineral form of PbO. As shown by Platteeuw and Meyer, SnO in the litharge structure is stable up to 300 °C, at which point it decomposes into a mixture of liquid tin and cassiterite.[5] The electronic structures of the stable phases of SnO and SnO_2 have been the subject of a recent study by Peltzer y Blancá *et al.*, motivated in part by the technological applications of SnO_2 in gas sensing and in the fabrication of transparent conductors.[6]

In addition to the stable phases, both oxides of tin undergo high-pressure transformations. An orthorhombic phase of SnO was observed at 2.5 GPa by Adams *et al.*,[7] and an orthorhombic phase of SnO_2 was found by Suito *et al.*[8] after quenching from a pressure of 15.8 GPa and a temperature of 800 °C. The high-pressure orthorhombic phase of SnO_2 is believed to have the same structure as α-PbO_2, which was refined by Hill in a neutron-scattering study of deposits formed on the plates of lead/acid batteries.[9] The orthorhombic structure has also been found in diamond-anvil SnO_2 experiments by Liu, who found that it was formed from a higher-pressure fluorite-type phase upon *release* of pressure.[10] A similar sequence of rutile-fluorite-orthorhombic phases was reported by Kusaba *et al.* in their shock-wave study of SnO_2, PbO_2, and $FeTaO_4$.[11] In a completely different type of experiment, but perhaps due to the same mechanism as in the shock-wave experiments, Lu *et al.* found electron-diffraction evidence for the orthorhombic phase of SnO_2 following the intense irradiation of cassiterite particles by an electron beam.[12] Lead and tin form a related group of oxide structures, and in a recent *in situ* x-ray scattering experiment of PbO_2 at pressures of up to 47 GPa, Haines *et al.* found a series of four high-pressure phases of PbO_2.[13] The second of these phases has a modified fluorite structure; on pressure release this phase reverted to α-PbO_2. In a similar set of diamond-anvil experiments on SnO_2, the orthorhombic phase was found beginning at 12.6 GPa during compression, but a greater fraction of this material (roughly 50%) was obtained on decompression.[14]

Our initial motivation for studying SnO_2 was the production of gas-sensing films;[15] we intended to prepare stable crystalline films with a relatively small (10–20 nm) grain size. Having deposited a set of samples consisting of amorphous SnO, we proceeded to heat them in air in order to crystallize the films in the stable (cassiterite) phase of SnO_2. The initial crystallization of these films in the litharge phase of SnO was not surprising, given the stoichiometry of the amorphous films. On the other hand, the subsequent formation of a high fraction of SnO_2 in the orthorhombic phase was as unexpected as it was unintentional. In the following sections of this paper we will detail the preparation of the orthorhombic-phase SnO_2 films and the x-ray scattering measurements which were used to confirm the sequential formation of three distinct crystalline phases. Finally, following a comparison to related thin-film experiments, we discuss the apparent existence of a transformation pathway to the orthorhombic phase through the litharge phase.

II. EXPERIMENTAL DETAILS

Si [001] substrates, approximately 12×6 mm^2 in size, were mounted on an unheated plate in a pulsed-laser deposition system, as shown in Fig. 1. Ablation was carried out using 532-nm radiation with typical pulse energies of 5 mJ distributed over a spot size of 0.5 mm, resulting in a typical fluence of 2.5 J/cm^2. The pulse rate was 5/s, and growth was carried out over 4 h, corresponding to a total of approximately 70 000 laser pulses. The sintered cassiterite ablation

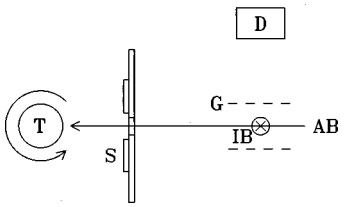

FIG. 1. Schematic diagram of the pulsed-laser deposition system. An ablation beam (AB) enters from the right, passes through an aperture in the substrate plate, and strikes a rotating and translating SnO_2 target (T). A plume of ablated material is emitted from the target and is deposited on substrates (S). Ablated species which pass through the aperture interact with the ionization beam (IB), which is normal to the ablation beam. After extraction by the grids (G), the ions pass through a drift tube and reach a detector (D).

target was rotated and translated during deposition in order to maintain a fresh target surface at the point of incidence of the ablation beam.

In situ time-of-flight mass spectrometry of the depositing species was carried out with 118.2-nm photoionization of the central portion of the ablated plume. Following extraction, ions traveled 118 cm to a dual-microchannel-plate detector. As detailed in Ref. 16, the predominant gas-phase species in the ablation plume were SnO and Sn_2O_2; in other words, the tin-containing species exhibit a one-to-one stoichiometry. No significant levels of SnO_2 were detected in the gas phase. This observation is consistent with the study of Platteeuw and Meyer,[5] who showed that although SnO is unstable as a solid, it is stable in the gas phase. Moreover, the subsequent crystallization of the deposited film in the litharge structure (below) is consistent with gas-phase species of composition $(SnO)_n$. Following deposition, film thicknesses were estimated by characterizing the sequence of interference fringes visible on the substrate plate and on the substrates. Two samples were prepared in an initial growth run, with an average thickness of approximately 400 nm. In a second growth run, four samples were made with an average thickness of approximately 130 nm.

X-ray scattering measurements were performed using a powder diffractometer in parafocusing Bragg-Brentano geometry[17] and a Cu tube source operated at 1 kW. A focusing graphite monochromator was mounted downstream of the sample on the detector arm, and 1° divergence slits were placed upstream and downstream of the sample. As shown below, the longitudinal resolution of the diffractometer at $q = 2.0$ Å^{-1} was approximately 0.012 Å^{-1}, where the scattering vector is given by $q = 4\pi \sin\theta/\lambda$. Lorentzian functions were used to fit the diffraction peaks, with positions, widths, and intensities returned by the fitting procedure. We estimate that at a typical scattering vector of 2.5 Å^{-1}, our measurements of peak positions are accurate to approximately 0.0025 Å^{-1}, resulting in an accuracy in measured d spacings of approximately 0.1%. In order to avoid the Si 004 substrate reflection, scans were run with the sample displaced by 1° from the specular condition, reducing the substrate scattering without significantly affecting the scattering from the deposited films. As an additional measure to eliminate spurious diffraction peaks, all illuminated portions of the sample holder were made from pure tungsten, resulting in a well-characterized background from which the sample scattering

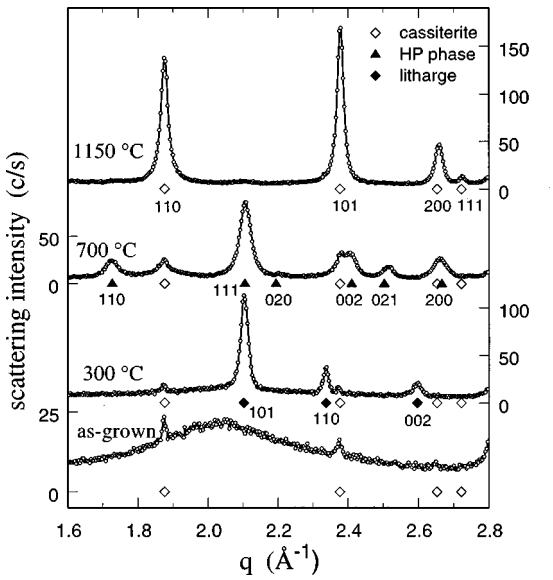

FIG. 2. X-ray scattering intensities for a sample at various stages of processing. The lower plot shows the as-grown sample, with most of the intensity contained in a broad feature corresponding to an amorphous structure. In addition, sharp peaks near the open diamonds indicate the presence of small quantities of cassiterite in the as-deposited film. The upper three curves are all plotted with the same vertical scale and show the evolution of three crystalline phases. At 300 °C, the film has crystallized in the litharge phase of SnO. After heat treatments reaching 700 °C, the sample has formed the orthorhombic high-pressure phase of SnO_2. Eventually, after a series of heating steps to 1150 °C, the orthorhombic phase is converted to cassiterite. Peak positions using lattice parameters from the literature are shown by open diamonds (cassiterite), filled triangles (the high-pressure phase), and filled diamonds (litharge). The same data files used in this figure were used in generating the data of Table I, and the most intense peaks of the crystalline phases are shown in Fig. 3. Data for the amorphous phase are replotted in Fig. 4, along with data from another sample.

could be distinguished clearly. In order to obtain satisfactory counting statistics, we used counting times of 40 s per point; scans running from 10° to 100° in 2θ with a step size of 0.05° took approximately 20 h to complete.

Heat treatments in air were carried out using a crucible furnace with the samples placed in an open quartz tube. Ramp rates were typically 700 °C per hour and soak times were usually 2–3 h. (Heating sequences for specific samples are given below.) Although the samples were heated as high as 1150 °C, we found no evidence of any interfacial reaction between the Si substrate and the films, presumably due to a combination of the immiscibility of tin and silicon[18,19] and the presence of the substrate native oxide as a barrier. The only visible change in those portions of the substrate uncovered by the films was a gradual color change to a darker shade of gray after heating to the highest temperatures.

III. RESULTS

Figure 2 gives an overview of the x-ray scattering results for one of the samples from the first growth run. Although data were taken with q ranging from 0.7 to 6.25 Å^{-1}, the

most significant changes in scattering intensity were found in the range shown in the figure. In addition to the measured scattering intensities, shown as small open circles connected by lines, the figure includes calculated peak positions for three crystalline phases, using the lattice parameters of Haines and Léger[14] for cassiterite, Suito *et al.*[8] for the high-pressure orthorhombic phase of SnO_2, and Pannetier and Denes[3] for the litharge phase of SnO.

In the as-prepared state (lower plot), a broad feature with a peak near $q=2.05$ Å^{-1} indicates that the film is amorphous. Sharp peaks near the open diamonds indicate the presence of cassiterite, but their integrated intensity is insignificant in comparison to that of the amorphous phase. The cassiterite peaks persist throughout the heat treatments, but they only begin to grow significantly above a temperature of 700 °C. It is likely that the cassiterite in the as-deposited film is composed of macroscopic fragments of the ablation target which are transferred to the substrate during the deposition process.

The sample was heat treated in a sequence of increasing temperatures and removed from the furnace after each step in order to perform *ex situ* x-ray measurements. There was no change in the scattering intensity after heating to 100 °C and then 200 °C, but after heating to 300 °C the film crystallized in the litharge phase of SnO (Fig. 2, second plot). The crystallization was not complete, however, since there was remaining intensity from the amorphous phase (not visible in Fig. 2), and also because the integrated litharge intensities are significantly lower than those of the phases which form subsequently.

The following heat treatments were performed at 50 °C intervals in temperature. During this process the litharge phase became disordered, as shown by peak broadening. The gradual development of a new phase was accompanied by the shifting, disappearance, and appearance of diffraction peaks. Eventually, by 700 °C, the scattering intensity of the new phase became that which is shown in the third plot of Fig. 2. As detailed below, the peak positions and relative intensities at this point agree very well with the values given by Suito *et al.* for the orthorhombic phase of SnO_2.[8] During continued heat treatments the orthorhombic phase was quite stable, in that it persisted in significant quantities even after heating the samples to temperatures above 1000 °C. Eventually, after heating to 1150 °C, the orthorhombic phase was almost completely replaced by cassiterite, as shown in the upper plot of Fig. 2.

Figure 3 contains expanded plots of the most intense peaks from each of the three crystalline phases, with the measured intensities shown as open circles and Lorentzian fitting functions shown as curves. In addition, a scan through the 111 peak of a Si powder standard is shown in the lower right. The Si peak, which is fit by a Gaussian function of width $\Delta q_{ins}=0.012$ Å^{-1}, is taken as representative of the instrumental resolution function at $q=2$ Å^{-1}. Since the SnO and SnO_2 peaks are significantly broader than the instrumental function, we approximate the intrinsic peak widths by assuming that the intrinsic and instrumental widths add in quadrature.[20] That is, we set $\Delta q_m^2=\Delta q_{int}^2+\Delta q_{ins}^2$, where Δq_m is the measured peak width, Δq_{int} is the intrinsic width, and Δq_{ins} is the instrumental width. Once the corrected widths are obtained, the average grain size corresponding to

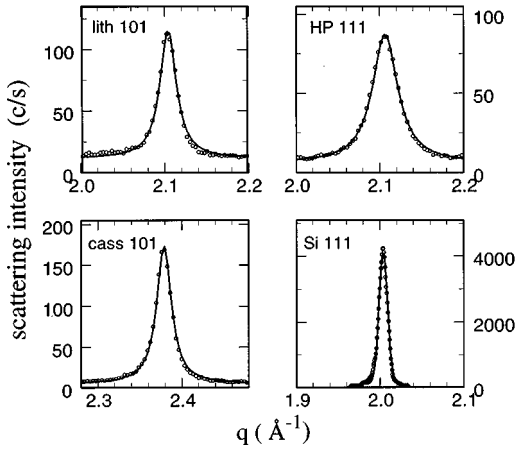

FIG. 3. Measured intensities (open circles) and Lorentzian fits (curves) for the strongest peaks in Fig. 2. The positions, widths, and intensities of these and other peaks are given in Table I. The lower right plot shows a scan through the 111 peak of a silicon powder standard, fit with a Gaussian function.

the crystalline phases can be approximated by the function $2\pi/\Delta q_{int}$.[20] Using the data of Fig. 3, we obtain grain sizes of 320 Å for the litharge phase, 180 Å for the high-pressure phase, and 360 Å for cassiterite.

In order to determine peak positions, intensities, and widths, Lorentzian fits were also performed for other relatively intense peaks, with the results shown in Table I. This table includes the measured peak positions, the corresponding d spacings (given by $d=2\pi/q$), and the agreement of the measured d spacings with values calculated using the same sources of lattice parameters as in Fig. 2. The table also includes the peak intensities and uncorrected widths, which are multiplied together in order to obtain estimates of relative integrated intensities. The last column of the table consists of relative intensities given by Suito *et al.* for the orthorhombic phase,[8] and the intensities listed in a standard diffraction database for the litharge phase[21] of SnO and the cassiterite phase[22] of SnO_2. For all three phases the agreement in peak positions between measured and previously published values is very good. The agreement in intensities is also good, given that thin films in general may exhibit a nonrandom orientation of crystallites. We conclude that the phase identification in these samples is unambiguous. If we assume that all of the film was converted to cassiterite after heating to 1150 °C (Fig. 2, upper plot), comparison of summed integrated intensities indicates that the yield of the high-pressure phase at 700 °C (Fig. 2, third plot) was approximately 50%.

The second sample from the first growth run was subjected to a similar set of heat treatments, except that temperature intervals of 25 °C rather than 50 °C were used between each step. The sequence of crystalline phases for this sample was similar to that of the first sample. We found no evidence of the formation of crystalline phases other than those discussed above. In particular, we found no evidence for an interfacial tin-silicon interaction, or a high-pressure phase of SnO, or for the formation of intermediate oxides such as Sn_3O_4.

During the second deposition run, films were deposited on four samples, using a second ablation target but otherwise under similar conditions. As mentioned above, visual obser-

TABLE I. Summary of diffraction data for the sample corresponding to Figs. 2 and 3. Indices prefixed by L indicate the litharge phase of SnO, HP indicates the orthorhombic high-pressure phase of SnO_2, and C indicates the cassiterite phase of SnO_2. The columns q_m, I_m, and Δq_m are the peak positions, intensities, and uncorrected widths derived from Lorentzian fits to the data used in Fig. 2. Column d_m contains the d spacing corresponding to q_m, and $(d_m - d_l)/d_l$ is the difference (in percent) between d_m and d-spacing values obtained from the published literature. For the purposes of comparing relative integrated intensities, column $I\Delta q_m$ contains the product of the peak intensity and peak width, normalized to a value of 100 at the strongest peak. Column I_l contains relative intensities from the literature.

Index	q_m (Å^{-1})	d_m (Å)	$\frac{d_m - d_l}{d_l}$ (%)	I_m (c/s)	Δq_m (Å^{-1})	$I\Delta q_m$ (norm.)	I_l (norm.)
L 001	1.294	4.857	0.4	7.1	0.022	6	10
L 101	2.104	2.987	−0.1	105.0	0.023	100	100
L 110	2.337	2.689	0.0	28.4	0.015	17	37
L 002	2.597	2.420	0.0	13.6	0.027	15	14
L 112	3.493	1.799	0.0	13.9	0.029	17	27
HP 110	1.726	3.640	0.0	17.7	0.044	26	30
HP 111	2.106	2.983	0.0	81.7	0.036	100	100
HP 021	2.513	2.500	0.4	12.1	0.038	15	20
HP 200	2.662	2.361	−0.2	21.2	0.044	31	10
HP 112	2.965	2.119	0.0	6.3	0.054	12	15
C 110	1.876	3.350	0.0	134.0	0.024	91	100
C 101	2.378	2.642	0.0	169.3	0.021	100	81
C 200	2.659	2.363	−0.2	43.8	0.025	31	24
C 211	3.566	1.762	−0.1	71.5	0.027	53	63
C 220	3.753	1.674	0.0	15.9	0.026	12	17
C 310	4.202	1.495	−0.2	10.3	0.033	10	13

vation of the interference patterns showed that the film thickness of the second set of samples was approximately one-third that of the first run. In Fig. 4 we compare the as-deposited amorphous-phase scattering for samples made in the two growth runs. The ratio of the peak intensities is approximately 3.5, close to the estimated ratio of film thicknesses. Since the samples from both runs have the same peak position and shape (Fig. 4), the scattering measurements do not reveal any difference in the structure of the amorphous component of the two sets of samples.

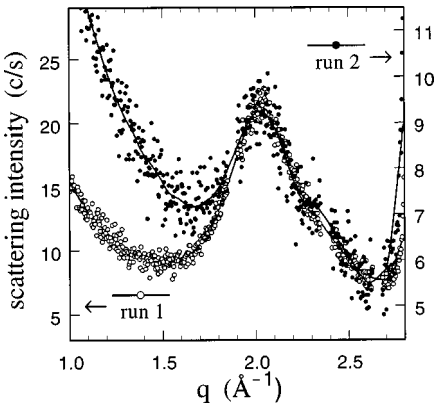

FIG. 4. Scattering intensities arising from the as-deposited amorphous phase, for samples from two separate growth runs, plotted with different vertical scales. Measured intensities are shown by filled and open circles; the curves were produced by a least-squares smoothing of the data. Sharp peaks from trace quantities of cassiterite in the as-deposited film (Fig. 2, lower plot) were removed by deleting all points within ± 0.05 Å^{-1} of the cassiterite 110, 101, and 200 reflections. The rise in intensities at small scattering vectors is background scattering from the main beam; the rise near 2.8 Å^{-1} is the shoulder of the tungsten 110 peak, originating in the sample holder.

A significant difference between the two sets of samples *was* found following heat treatments: the samples produced in the second growth run did not crystallize in the litharge phase of SnO, even when subjected to the same heat treatments as the first sample from the first growth run. Instead, peaks corresponding to cassiterite gradually emerged out of the broad amorphous-phase scattering. In summary, the sequence of structures for samples in the first growth run was (i) amorphous SnO, (ii) litharge-phase SnO, (iii) orthorhombic SnO_2, and (iv) cassiterite. Samples from the second run went directly from an amorphous structure to cassiterite, with no evidence of an orthorhombic component.

We have not identified an obvious cause of the differences between the two sets of samples. A different ablation target was used, thus it is possible that variations in the surface topology of the targets led to differences in ablation yields and deposition rates. On the other hand, mass spectrometry during the second deposition run showed a distribution of gas-phase species similar to that of the first run. We see no reason why a reduced film thickness *per se* would inhibit the crystallization of the film in the litharge structure. Perhaps the difference may lie in the stoichiometry of the as-deposited samples: a modest excess of oxygen in the second set could prevent the crystallization of SnO, but would be undetectable in scattering measurements such as those of Fig. 4. If, as we speculate below, the litharge structure serves as a pathway to the crystallization of the orthorhombic

phase, slight variations in the initial stoichiometry could preclude the formation of the high-pressure phase.

IV. DISCUSSION

The formation of a high-pressure phase in a polycrystalline film is fairly unusual, but in the case of tin oxide we can refer to several related experiments. Kaplan *et al.* have observed electron and x-ray-diffraction features corresponding to the orthorhombic phase of SnO_2 in films produced by the deposition of ionized tin atoms in the presence of oxygen.[23] Although the high-pressure phase was not the main focus of their study, they reported traces of this phase in films deposited on heated substrates and after heat treating amorphous films deposited on lower-temperature substrates. They suggested that the formation of the high-pressure phase in the first case may be due to the energetic nature of ion deposition on a biased substrate, and that in the second case the formation may be due to a relatively high density of the amorphous phase. In a different study of ultrafine 5-10 nm tin oxide powders, Shek *et al.* detected orthorhombic SnO_2 in x-ray scattering measurements of powders which were heat treated in air.[24] On the other hand, they found that the high-pressure phase was suppressed when the annealing was done in oxygen. A third set of related experiments was carried out by Kraševec *et al.*, who performed electron-diffraction measurements on films prepared by the oxidation of epitaxial single-crystal films of litharge-structure SnO.[25] In a subsequent paper,[26] Prodan *et al.* showed that the oxidized litharge structure in fact consisted of the orthorhombic phase of SnO_2. It is significant that the orthorhombic-phase diffraction pattern corresponded to two domains, rotated by 90° with respect to each other, each with a specific orientation with respect to the SnO structure.[25] In other words, the orthorhombic phase was formed through a process of *epitaxial* oxidation of the litharge structure.

The thin-film and powder experiments indicate that the orthorhombic phase of SnO_2 can be synthesized through a variety of routes which are not explicitly associated with high pressures. Although Prodan *et al.*[26] invoked the effects of epitaxial strain at the film-substrate interface, the experiments of Kaplan *et al.*[23] and our experiments were carried out on randomly oriented polycrystalline films, where epitaxial strains should be less important. Even though one could invoke strains during the oxidation of polycrystalline films which are constrained by adhesion at the substrate interface, Shek *et al.*[24] found the orthorhombic phase in unconstrained powders. In addition, we found no obvious indication of strains in our films, since the peak positions which we observed were close to the values reported for unstrained samples (Table I).

It is our opinion that the key ingredient in our synthesis of orthorhombic-phase SnO_2 is not compressive stress in the films, but the formation of the litharge phase of SnO as a precursor. Evidence for this conjecture is found in our x-ray measurements on samples heat treated at temperatures between 300 and 700 °C, which show that the nucleation of the high-pressure phase coincides with the disruption of the litharge structure. Another consistent observation is that no trace of the orthorhombic phase was found in our second set of samples, where the litharge phase was absent. The observation of Shek *et al.*[24] that formation of the high-pressure phase is suppressed in oxygen-rich environments is also consistent with this view, since the rapid oxidation of SnO could inhibit its action as a precursor. Finally, we find that the epitaxial relationship[25] between the litharge structure and the orthorhombic phase is a clear indicator of the probable importance of litharge-phase SnO as a transformation route.

Our results are not in disagreement with the high-pressure experiments which indicated that the modified-fluorite phase serves as a precursor to the orthorhombic structure during decompression.[10,11,14] Instead, we suggest that the litharge phase plays a role in an *alternative* transformation route. (This route would not have been detected in the high-pressure experiments since in that case the tin-oxygen stoichiometry is fixed at one to two.) The obvious experiment which one might try in probing the alternate route is the modification of bulk samples of litharge-phase SnO by appropriate heating steps in controlled oxygen environments. As a test of the possible role of film stress in nucleation of the orthorhombic phase, one could deposit amorphous SnO films on sets of substrates with different thermal-expansion coefficients, in order to vary the film-substrate interface stress during heat treatments. Another set of experiments, motivated by the known relationships between high-pressure oxide phases of lead and tin, would involve the oxidation of thin films of litharge.

Although the high-pressure experiments have been very illuminating, experiments such as ours indicate that there are some interesting unsolved questions relating to the formation of metastable oxides. Aside from the question of alternate transformation routes, thin-film experiments present the following opportunity: given the stability and the relatively high fraction of orthorhombic SnO_2 which we have observed, it should be possible to produce samples which are suitable for optical and transport measurements, which to our knowledge have yet to be performed on this material.

ACKNOWLEDGMENTS

We acknowledge a series of helpful discussions throughout the course of this work, primarily with J. Hossenlopp, M. Gajdardziska-Josifovska, P. Lyman, A. R. Day, and S. R. Swaminathan. Important technical support was provided by C. Pugh-Smith, N. Schook, and L. Mursec. Financial support was provided by the Arnold and Mabel Beckman Foundation (S.A.R.), the Center for Sensor Technology at Marquette University (F.J.L. and S.A.R.), the N.S.F. CAREER program, Grant No. NSF CHE9702803 (S.A.R.), and the Wehr Foundation (F.J.L.).

[1] *Dana's Manual of Mineralogy*, 15th ed., revised by Cornelius Hurlbut (Wiley, New York, 1941).
[2] Walter J. Moore and Linus Pauling, J. Am. Chem. Soc. **63**, 1392 (1941).
[3] J. Pannetier and G. Denes, Acta Crystallogr., Sect. B: Struct. Crystallogr. Cryst. Chem. **36**, 2763 (1980).
[4] F. Izumi, J. Solid State Chem. **38**, 381 (1981).
[5] J. C. Platteeuw and G. Meyer, Trans. Faraday Soc. **52**, 1066 (1956).
[6] E. L. Peltzer y Blancá, A. Svane, N. E. Christensen, C. O. Rodríguez, O. M. Cappannini, and M. S. Moreno, Phys. Rev. B **48**, 15 712 (1993).
[7] David M. Adams, Andrew G. Christy, Julian Haines, and Simon M. Clark, Phys. Rev. B **46**, 11 358 (1992).
[8] K. Suito, N. Kawai, and Y. Masuda, Mater. Res. Bull. **10**, 677 (1975).
[9] Roderick J. Hill, Mater. Res. Bull. **17**, 769 (1982).
[10] Lin-Gun Liu, Science **199**, 422 (1978).
[11] Keiji Kusaba, Kiyoto Fukuoka, and Yasuhiko Syono, J. Phys. Chem. Solids **52**, 845 (1991).
[12] Bin Lu, Changsui Wang, and Yuheng Zhang, Appl. Phys. Lett. **70**, 717 (1997).
[13] J. Haines, J. M. Legér, and O. Schulte, J. Phys.: Condens. Matter **8**, 1631 (1996).
[14] J. Haines and J. M. Léger, Phys. Rev. B **55**, 11 144 (1997).
[15] Jeanne M. Hossenlopp, F. J. Lamelas, Kenneth Middleton, Jeffrey A. Rzepiela, Jason D. Schmidt, and Aleksandar Zivkovic, Appl. Organometal. Chem. **12**, 147 (1998).
[16] S. A. Reid, Chem. Phys. Lett. **301**, 517 (1999).
[17] L. A. Aslanov, G. V. Fetisov, and J. A. K. Howard, *Crystallographic Instrumentation* (Oxford University Press, Oxford, 1998).
[18] W. B. Pearson, *A Handbook of Lattice Spacings of Metals and Alloys* (Pergamon, New York, 1958).
[19] Max Hansen, *Constitution of Binary Alloys* (McGraw-Hill, New York, 1958).
[20] A. Guinier, *X-Ray Diffraction in Crystals, Imperfect Crystals, and Amorphous Bodies* (Freeman, San Francisco, 1963).
[21] Powder Diffraction File, Card No. 6-0395 (International Centre for Diffraction Data, Swarthmore).
[22] Powder Diffraction File, Card No. 21-1250 (International Centre for Diffraction Data, Swarthmore).
[23] L. Kaplan, A. Ben-Shalom, R. L. Boxman, S. Goldsmith, U. Rosenberg, and M. Nathan, Thin Solid Films **253**, 1 (1994).
[24] C. H. Shek, J. K. L. Lai, G. M. Lin, Y. F. Zheng, and W. H. Liu, J. Phys. Chem. Solids **58**, 13 (1997).
[25] V. Kraševec, A. Prodan, M. Hudomalj, and S. Sulčič, Phys. Status Solidi A **87**, 127 (1985).
[26] A. Prodan, N. Vene, F. Sevšek, and M. Hudomalj, Thin Solid Films **147**, 313 (1987).